Pergamon

PII: S0301-9322(96)00085-7

Int. J. Multiphase Flow Vol. 23, No. 5, pp. 865–884, 1997

Printed in Great Britain
0301-9322/97 $17.00 + 0.00

ENTRAINMENT BY LIGAMENT-CONTROLLED EFFERVESCENT ATOMIZER-PRODUCED SPRAYS

J. J. SUTHERLAND, P. E. SOJKA and M. W. PLESNIAK

Thermal Sciences and Propulsion Center, School of Mechanical Engineering, Purdue University, West Lafayette, IN 47907-1003, U.S.A.

(Received 24 June 1996; in revised form 17 November 1996)

Abstract—Entrainment of ambient air into sprays produced by a new type of effervescent atomizer is reported. Entrainment data were obtained using a device similar to that described previously. Entrainment data were analyzed using a previous model, together with measured momentum rate data that were also acquired as part of this study. The analysis shows that entrainment by sprays produced using this type of atomizer is predicted to within about 35% by the expression $E = \dot{m}_e/x\sqrt{\rho_e M_o}$, where $\dot{m}_e$ is the entrained gas mass flow rate, x is the distance along the spray axis measured from the dispenser exit orifice, ρ_e is the density of the entrained air, M_o is the spray momentum rate at the exit orifice, and E is the experimentally determined entrainment number whose value is 0.15 ± 0.056 (2σ). © 1997 Elsevier Science Ltd.

Key Words: sprays, entrainment, experimental, ligament-controlled effervescent atomizer

1. INTRODUCTION

Effervescent atomization is characterized by actively introducing gas bubbles into a liquid stream immediately upstream of an exit orifice, thereby forming a two-phase flow. This allows efficient transfer of energy between the atomizing gas and the liquid. The result is a high quality spray (i.e. small mean drop size) produced at air-to-liquid mass flow rate ratios (ALRs) substantially lower than most atomizers. A typical "conventional" effervescent atomizer is shown in figure 1.

A number of investigators have studied sprays produced by effervescent atomizers. They have been concerned almost exclusively with atomizer performance, i.e. mean drop size, and have reported their results in terms of the spray Sauter mean diameter (SMD or, equivalently, D_{32}).

Early studies focused on the relationship between atomizer performance and nozzle geometric design features with Lefebvre *et al.* (1988) reporting little influence of exit orifice diameter on mean drop size and Wang *et al.* (1987) showing that mean drop size was insensitive to gas injector geometry. Subsequent studies were concerned with how the two-phase flow within the atomizer controlled performance—Roesler and Lefebvre (1989) investigated the role of gas bubbles while Whitlow and Lefebvre (1993) studied sprays produced by both annular and multihole exit orifice designs.

Later work reported performance when spraying high viscosity and non-Newtonian fluids. Buckner and Sojka (1993) showed viscosity had a limited effect on mean drop size for high viscosity fluids, and suggested that fluid viscoelasticity was the key factor in controlling mean drop size. The importance of viscoelasticity was supported by the work of Geckler and Sojka (1996).

More recent work resulted in analytical models able to predict mean drop size. Lund *et al.* (1993) used high speed photography to capture the near atomizer fluid breakup processes that result in droplet formation and observed an annular band of ligaments breaking up into drops. The results of Santangelo and Sojka (1995) supported the conclusions of the Lund *et al.* (1993) study, and also demonstrated that a transition from annular to slug/bubble flow is directly responsible for the marked increase in mean drop size that is observed when the air-to-liquid mass flow ratio is reduced.

The observations of Lund *et al.* (1993) and Santangelo and Sojka (1995) were used to design the ligament-controlled effervescent atomizer shown in figure 2. It differs from earlier effervescent

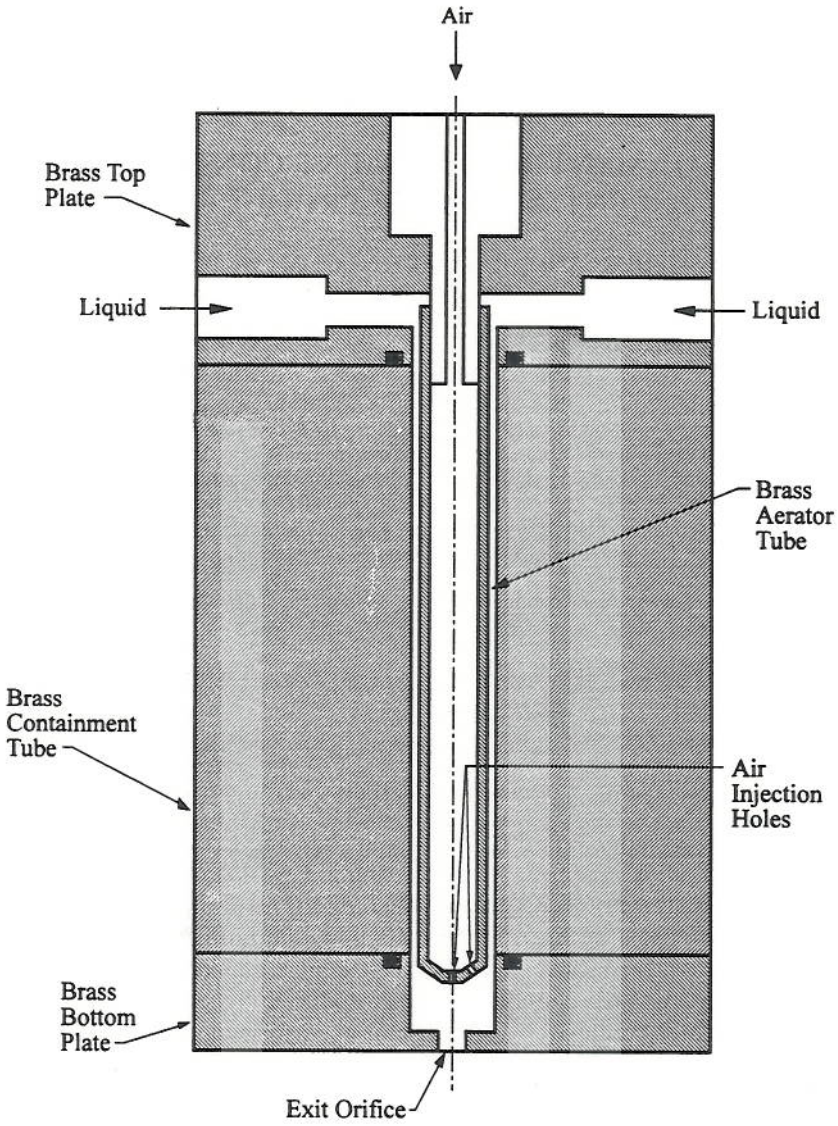

Figure 1. Conventional effervescent atomizer.

atomizers because a porous plug was inserted into the exit orifice. The plug, made of sintered plastic with pores nominally 37 μm in diameter, allows sprays to be formed at ALRs as low as 0.75%. Spray performance is described by Sutherland (1996).

All of the studies cited above have been concerned with spray performance, i.e. mean drop size. One topic of spray research which has not been studied in detail is entrainment. Entrainment, for the purposes of this discussion, is defined as the quantity of ambient gas which is drawn in through the interface of a spray as it expands downstream of the nozzle. It is the result of momentum transfer, from both liquid drops and any atomizing gas used, to the ambient air surrounding the spray.

Entrainment has important implications in many engineering applications. In consumer product sprays, the entrained mass flow rate has a cause and effect relationship with carrier liquid evaporation. In combustion applications such as gas turbines and diesel engines, entrainment has a significant effect on the local equivalence ratio and, therefore, a direct impact on NO_x formation. In furnaces, entrainment has a large impact on droplet residence time since higher entrainment rates lead to greater rates of spray deceleration and, therefore, slower moving drops. Entrainment is also important in spray drying, where the goal is to remove as

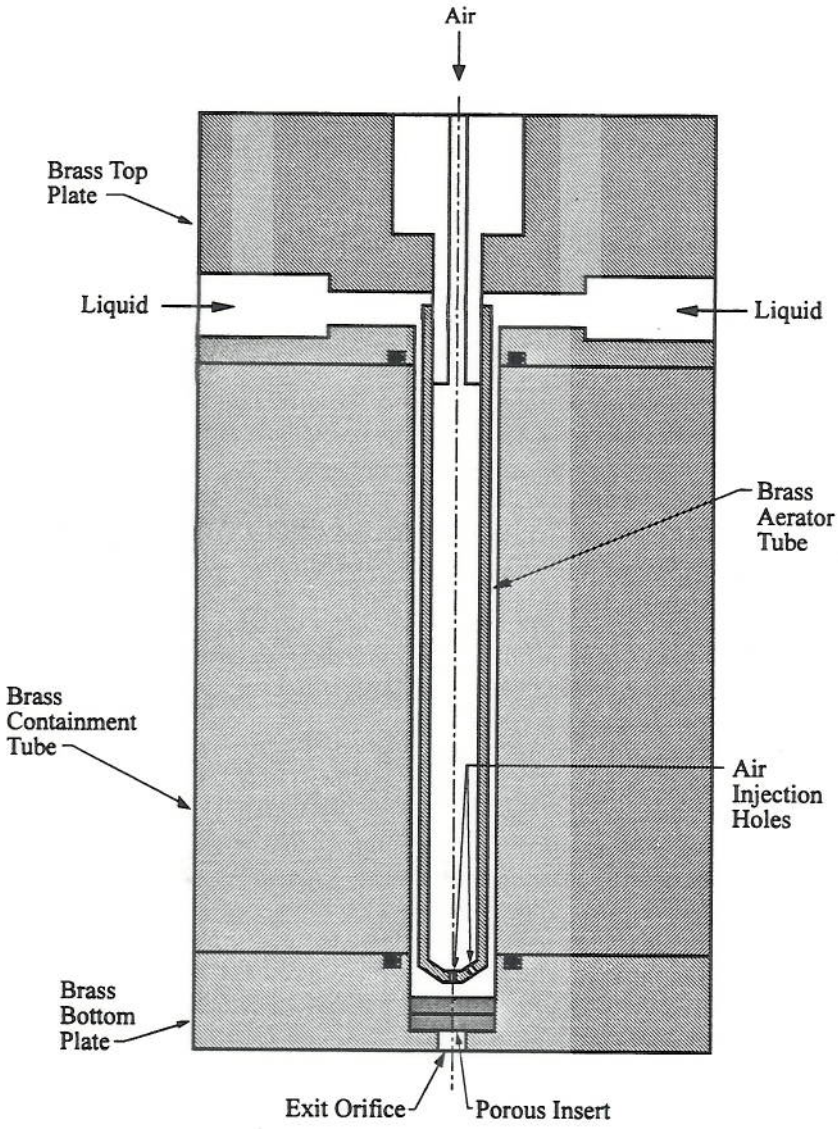

Figure 2. Ligament-controlled effervescent atomizer.

much liquid as possible from a droplet during the drying process. Finally, entrainment can influence the finish quality of painted or coated surfaces through both transfer efficiency and solvent evaporation.

A key to understanding entrainment is the ability to measure it. Three methods are common: (i) experimentally measuring the velocity profile of the entrained air and then integrating it over a control volume that encompasses the spray; (ii) measuring the global entrainment rate; and (iii) numerically simulating the two-phase spray field. Studies that have used these techniques, and that are relevant to the current work, are summarized below.

Binark and Ranz (1958) measured velocities outside the spray using a constant-resistance hot wire anemometer and inside the spray using an impact-static probe. Data were used to develop an expression that yielded induced air velocities for a set of homologous nozzles. Unfortunately, their expression is of limited use for estimating entrainment into sprays because atomizer-specific experimental data are necessary in order to apply their model to other types of atomizers. Binark and Ranz (1958) also developed a theoretical model that yielded results within an order of magnitude of their experimental data. However, it required the assumption that the velocity of the drops was constant and equal to the injection velocity. If this assumption were correct, no transfer

of momentum would occur between the drops and the surrounding air and, thus, no air would be entrained.

Rasbash and Stark (1962) correlated spray entrainment in terms of "reaction at the nozzle", or the force exerted on a flat obstacle oriented normal to the spray axis. The fact that Rasbash and Stark (1962) present their results as an empirical correlation suggests that their expression is applicable only to sprays formed using their type of atomizer.

Briffa and Dombrowski (1966) measured entrained air velocity by seeding the air in and around a flat spray with lycopodium powder and taking double-flash (microsecond duration) photographs. Air velocities inside the spray were measured assuming the air velocity was tracked by the 15 μm diameter droplets. A model was developed which demonstrated a linear relationship between entrained mass flow rate and axial distance. However, a non-linear relationship was observed experimentally.

Benatt and Eisenklam (1969) used the Ricou and Spalding (1961) method to measure global entrainment and compared results obtained to predictions from a model based on their knowledge of the liquid sheet breakup process, spray dynamics, momentum loss calculations, and induced gas flow observations. The expected linear scaling of entrainment with axial distance was observed, and experimental results confirmed their theory. However, the theoretical proportionality constant was lower than the experimental value. Benatt and Eisenklam's (1969) model is restricted to pressure-swirl atomizers, since it relies on calculations based on a particular breakup process.

Tishkoff (1985) studied air entrainment into two different pressure-swirl atomizers by visualizing the entrained air flow patterns using helium jet seeding and measuring velocities using a constant temperature hot-wire anemometer. He developed a correlation for the entrainment number, which is limited to pressure-swirl atomizer produced sprays.

MacGregor (1991) developed a simple model based on jet momentum rate and the drag on spherical droplets and then used a Ricou and Spalding (1961) device to test it. Experimental results obtained from two nozzles show a linear relationship with inlet mass flow rate. However, the gradient of the experimental data implies that there exists a critical mass flow rate below which little or no entrainment occurs, suggesting little or no jet breakup is occurring under these conditions, and predictions did not agree with experimental results. Nonetheless, MacGregor (1991) used his model to demonstrate the effects of drop size distribution parameters and noted that entrainment rates were a linear function of axial distance for drops having diameters greater than 1000 μm, that entrainment rates fell off at large axial distances for smaller drops, and that entrainment rates were relatively insensitive to the width of the drop size distribution.

Boysan and Binark (1979) and Rothe and Block (1977) performed numerical simulations in order to predict induced air flows into sprays. Boysan and Binark (1979) assumed a Rosin–Rammler drop size distribution and numerically solved the partial differential equations for stream function and vorticity transport coupled with the ordinary differential equations of spray motion. Good agreement was observed upon comparison of predicted and measured air velocities. However, this agreement is misleading due to the incorporation of adjustable parameters into their model. These parameters would have to be determined for each new type of spray.

Rothe and Block (1977) were interested in the cone angle contraction due to entrained gas flow that was noted earlier by Binark and Ranz (1958). They numerically solved equations for drag, axial momentum, and drop trajectory in order to calculate the induced air velocity and amount of spray contraction. Comparisons of model predictions with experimental data of previous researchers were presented. Again, the level of agreement between model predictions and experimental results is misleading due to the use of fitting parameters in their analysis.

Ruff *et al.* (1989) were among the first to consider entrainment in the dense region of the spray, i.e. where the liquid is breaking up. Their analysis was based on the assumption of a locally homogenous flow (LHF). Mean streamwise and radial entrainment velocities were obtained using laser Doppler anemometry near the edge of the spray. These velocities were then integrated to provide experimental entrainment rates. Predicted values were greater than measured values in all cases. This is because entrainment rates are strongly related to flow properties near the edge of the spray. Unfortunately, this is also a dilute region of the spray where the LHF model over predicts quantities such as the entrainment rate.

Until recently, no studies addressing entrainment into effervescent sprays had appeared in the literature. Bush and Sojka (1994) were the first to study entrainment in such sprays, using an injector similar to that shown in figure 1. As such, they were the first to study entrainment in two-phase jets characterized by velocity slip between the two phases at the nozzle exit. Bush and Sojka (1994) developed a two-phase model analogous to that of Ricou and Spalding (1961) that was based on dimensional analysis and the conservation of momentum. A Ricou and Spalding (1961) device was then used to measure entrainment rates. They found that "conventional" effervescent sprays entrain air similar to other sprays and single-phase gas jets, in that the normalized entrainment rate scales linearly with the dimensionless axial distance. However, their results also show that "conventional" effervescent sprays are not characterized by a single entrainment number, as are their single-phase gas jet counterparts, instead requiring scaling by liquid density and nozzle diameter. Recent work by Luong (1996) suggests this lack of a single value for entrainment number is due to unsteadiness inherent in conventional effervescent sprays.

This review of the spray entrainment literature demonstrates that previous work cannot be directly applied to ligament-controlled effervescent atomizer produced sprays. Consequently, the current study extends previous work to this important class of atomizer by answering the practical question "At what rate does a ligament-controlled effervescent atomizer produced spray entrain surrounding air?" The current study also answers a question of more fundamental importance, i.e. "Can entrainment by sprays having initial inter-phase velocity slip be modeled using the momentum-rate approach first suggested by Ricou and Spalding (1961) for gas jets?"

2. EXPERIMENTAL APPARATUS

As mentioned previously, work by Lund *et al.* (1993) and Santangelo and Sojka (1995) indicated that atomizer performance could be improved (i.e. D_{32} reduced) by producing smaller ligaments at the injector exit. The current atomizer, shown schematically in figure 2, achieves that goal through use of a porous disk located at the exit orifice. As can be seen in figure 2, the atomizer consists of a top plate, a containment tube, an aerator tube, and an exit orifice plate. Liquid is fed into the side of the atomizer and flows through an annular gap between the containment and aerator tubes. Air is injected into the liquid through two holes located at the tip of the aerator tube. The resulting two-phase flow passes through a porous medium before leaving through the exit orifice.

The aerator tube is 133 mm long, has a diameter of 3.2 mm, and passes through a Cajon "Ultra-torr" vacuum fitting threaded into the atomizer top plate to allow for fine adjustment of its position relative to the exit orifice.

The containment tube has an outside diameter of 50.8 mm and an inside diameter of 3.7 mm. The gap between the aerator and containment tubes was sized at 0.3 mm in order to create a downward liquid velocity sufficient to counteract air bubble buoyancy.

The exit orifice plate has a diameter of 50.8 mm and a thickness of 3.2 mm. A 4.1 mm diameter blind hole with a depth of 2.95 mm is used to hold the porous medium in place just upstream of the exit orifice. The exit orifice diameter is 0.38 mm and its length is 0.25 mm. A very short exit length was used in order to minimize coalescence of either bubbles inside the atomizer itself or of liquid ligaments formed in the porous medium.

The porous medium, obtained from Porex Technologies, is a Polyvinylidene Fluoride (PVDF) disc that has a diameter of 4.1 mm, a thickness of 1.0 mm, a nominal pore size of 37 μm, and an average pore volume of 40%. The pore volume is the ratio of the volume of the void space to the total volume of the medium.

Since the porous medium serves to control the diameter of ligaments that eventually form drops (Sutherland 1996), the choice of pore size is important. This particular medium was chosen by trial-and-error as one that would provide acceptable spray performance (a mean drop size less than 70 μm) while requiring a minimal operating pressure (nozzle supply pressure less than 800 kPa) for ALRs below 1%.

The nozzle operates using supplies of metered atomizing air and liquid. The air flow rate was monitored using a Matheson 602 rotameter with a stainless steel float and regulated using a Nupro B-SS2-D needle metering valve. Rotameter calibration was performed by collecting, timing, and

measuring the volume of gas passing through it at several different settings. Due to the air mass flow rates involved in this study (as low as 0.0025 g/s), the air was collected and measured in an inverted graduated cylinder placed in a water bath. A straight line was fit to the data and yielded a coefficient of determination (r^2) of 0.991.

The liquids were supplied from a reservoir, with mass flow rates for the low viscosity fluids monitored using a Matheson 604 rotameter with a stainless steel float and those for the high viscosity fluids measured using a Matheson 605 rotameter with a stainless steel float. Flow rates were regulated using a needle valve. The liquid rotameters were calibrated by collecting, timing, and measuring the volume of liquid passing through the rotameter at several different settings. Straight lines were fit to the data, yielding coefficients of determination (r^2) greater than 0.95 for all cases.

The atomizer can deliver liquid mass flow rates of between 0.5 and 1.0 g/s. It can operate at air–liquid ratios by mass (ALRs) of 0.5% and above. Data presented here are restricted to 0.5 and 0.6 g/s and $0.75 \leq \text{ALR} \leq 3.75\%$.

Global entrainment rates were measured using a device similar to the one developed by Ricou and Spalding (1961). Their device consisted of a cylindrical housing that enclosed a nozzle mounted to a back plate. Entrained gas was injected into the cylinder and forced to pass through a porous inner cylinder before mixing with the jet. The porous boundary served to create a uniform radial velocity profile for the entrained gas. A mask of the same diameter as the jet was placed at the cylinder exit under zero pressure drop conditions. This mask helped to prevent any inflow or outflow of gases that might affect the entrainment measurement. By supplying entrained gas such that the pressure differential across the exit mask is zero, the entrained mass flow rate may be measured. Since there are no pressure gradients in an ambient environment, the flow conditions of a jet spraying into ambient air are duplicated when the pressure differential across the mask is zero.

The entrainment device discussed above was successfully adapted by Bush (1994) to measure entrainment rates of effervescent sprays. A schematic of the device is shown in figure 3, while exact design specifications may be found in Bush (1994).

A key to adapting the device to sprays was proper sizing of the exit mask. To accomplish this, twelve square Plexiglas plates were constructed, each with a hole bored in its center. Hole diameters range from 13 to 152 mm, which allowed rapid fitting of the proper mask size at each spray operating condition. A proper size is achieved when the exit mask is large enough to allow the spray to pass through (i.e. no droplets striking the mask), but not so large as to leave a gap between the edge of the spray and the mask. Once the proper mask is installed, data acquisition consists of adjusting the entrained air mass flow rate such that there is no pressure gradient across the exit mask and then recording the corresponding rotameter setting. The entrained air mass flow rate is calculated from this reading.

The pressure differentials across the exit mask were monitored using a MKS model 229HD differential pressure transducer with a Newport 4–20 mA, 3.5 digit process indicator. This enabled measurements of ± 1 torr (135 Pa) full scale with 1 mtorr (135 mPa) resolution.

The entrained air mass flow rates were measured using an Omega Engineering FL-1503A rotameter and controlled by a needle valve. The rotameter was calibrated using an American Meter DTM-115 volumetric gas flow meter and a MicroMotion Model D25 electronic mass flow meter. A straight line was fit to the data, yielding a coefficient of determination (r^2) of 0.999.

Entrainment by a 1 g/s air jet was measured at several axial positions and compared to results obtained by Ricou and Spalding (1961) in order to check the performance of the entrainment device. The data were reduced to the form reported in Ricou and Spalding (1961)

$$E = \frac{\dot{m}_e}{x\sqrt{\rho_e M_o}} \qquad [1]$$

where $\dot{m}_e$ is the entrained gas mass flow rate, x is the axial distance from the nozzle, ρ_e is the entrained gas density, and M_o is the spray exit momentum rate. E is the dimensionless entrainment number, as defined by Ricou and Spalding (1961), and determined by them to be 0.282 ± 0.015 for high Reynolds number air jets ($\text{Re}_d > 25{,}000$).

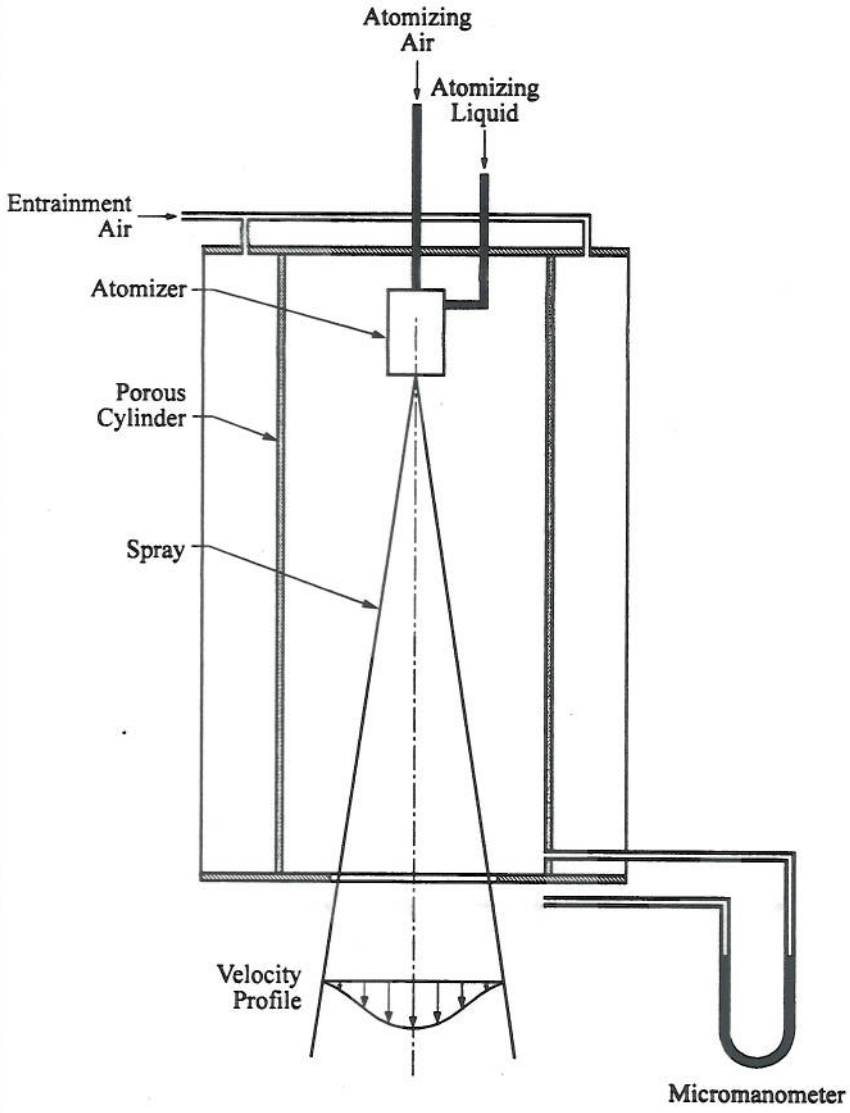

Figure 3. Entrainment device.

Data taken using the entrainment device described above are shown in figure 4. The results are presented as normalized entrainment versus normalized axial distance. Normalized entrainment is defined as the entrained gas mass flow rate, $\dot{m}_e$, divided by the liquid mass flow rate at the atomizer exit, $\dot{m}_L$, while normalized axial distance is defined as the distance along the spray axis, x, divided by the atomizer exit orifice diameter, d_o. The linear fit for the data shown in this plot has a coefficient of determination (r^2) of 0.978 and results in an entrainment number of 0.232 ± 0.010, a value within 18% of that reported by Ricou and Spalding (1961).

In order to obtain entrained air flow measurements characteristic of a spray operating in an ambient environment, it is critical that the entrainment device does not interfere with the structure of the spray. To confirm this, an Aerometrics Phase/Doppler Particle Analyzer (P/DPA) was used to collect radial velocity and drop size profiles for the case where the nozzle was operating inside the entrainment device and for the corresponding case where the nozzle was operating in the open environment. These two scenarios were compared for all liquids sprayed in this study at several liquid mass flow rates, air-to-liquid mass flow ratios, and axial positions.

Figure 5 shows the mean velocity profile for an 0.080 Pa-s viscosity, 0.030 Pa-m surface tension spray operating at a liquid flow rate of 0.8 g/s and an ALR of 10%. It is representative of data obtained for all fluids and operating conditions. Note that the average velocities for the atomizer

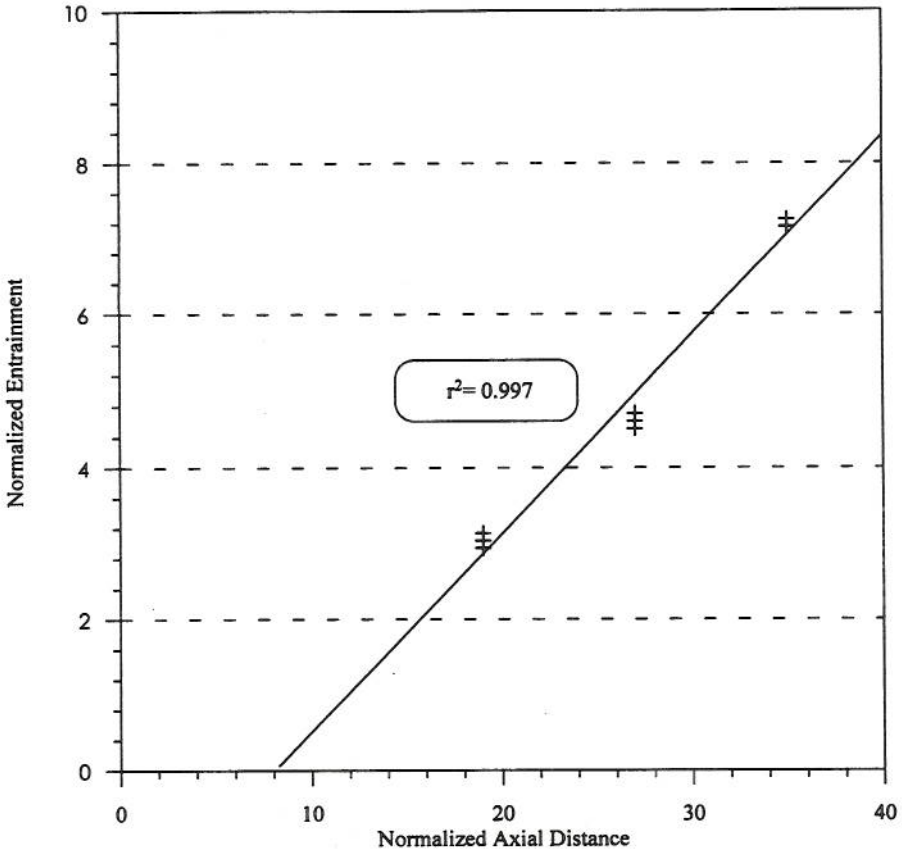

Figure 4. Entrainment data for a 1.0 g/s turbulent air jet, obtained using the entrainment device of figure 3.

operating with the entrainment device are in excellent agreement with the average velocities for the atomizer operating without the device.

Figure 6 shows the number averaged drop size (D_{10}) profiles for the same spray used in the collection of data for figure 5. This figure is also representative of data obtained for all fluids and operating conditions. Note that the average drop sizes for the atomizer operating with and without the entrainment device are in excellent agreement. This level of agreement in the drop velocity and size profiles was observed for all cases studied, indicating that the entrainment device does not significantly alter the structure of the effervescent spray. We therefore conclude that entrainment data obtained using the device are representative of entrainment in the ambient environment when the differential pressure boundary condition at the device exit is satisfied.

A number of previous spray entrainment studies have demonstrated the importance of jet momentum rate on entrained gas flow rates. Bush *et al.* (1996) constructed a device for determining the axial momentum of two-phase jets based on the design of Deichsel and Winter (1991). That probe was used in this study. A summary of its principles and operation is provided below.

The momentum rate of a spray is measured by a converting the axial flow to a radial flow by spraying against a deflection cone whose contour is obtained from the equation of streamlines for an incompressible, axisymmetric, stagnation point flow (White 1991). It is easily shown that the amount of reaction force needed to hold the cone in place is equal to the momentum rate of the spray.

For this study, the deflection cone was mounted on a cantilevered beam. When the spray is directed at the cone, the beam is deflected, resulting in a strain at the base. This strain can be measured with strain gages and appropriate signal conditioning hardware. Bush *et al.* (1996) describe the design details of the deflection cone, the strain gage beam, and the signal conditioner. A schematic of the momentum rate probe is shown in figure 7.

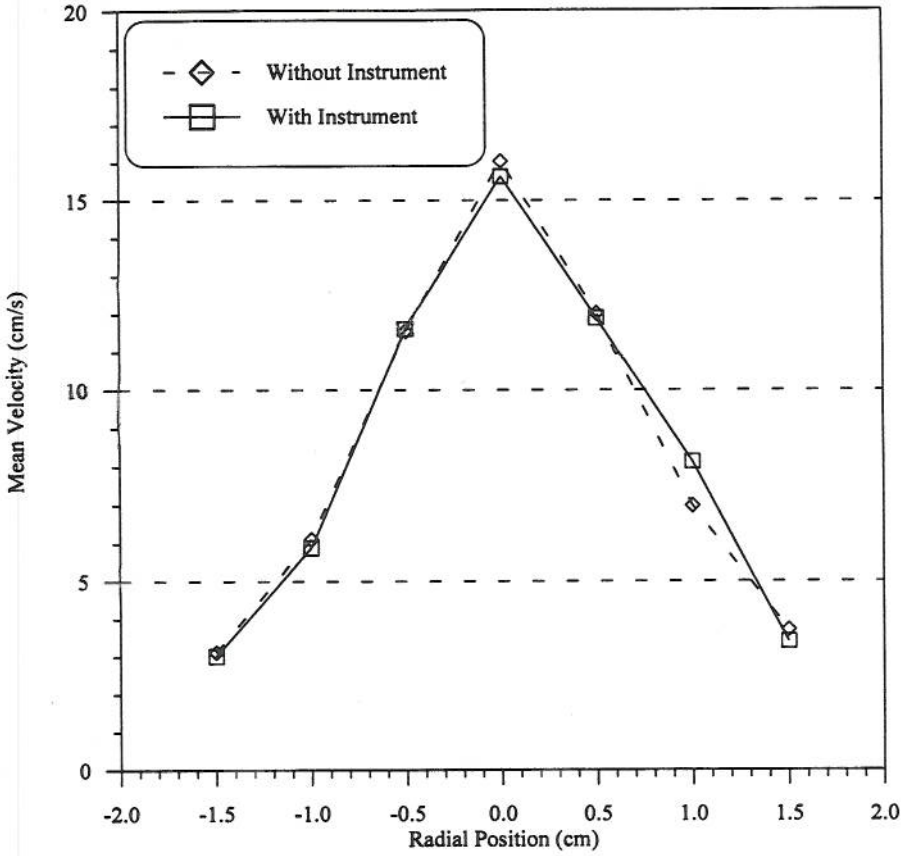

Figure 5. Radial droplet velocity profile for a ligament-controlled effervescent atomizer produced spray formed from a 0.080 Pa-s viscosity, 0.030 Pa-m surface tension fluid.

A liquid jet with a known velocity profile, whose momentum rate is easily calculated, was used to calibrate the momentum rate probe. By operating the atomizer with only liquid at several mass flow rates, a calibration curve of momentum rate vs probe voltage output was produced. The momentum rate was calculated based on either a fully developed or slug flow velocity profile, depending on the viscosity of the fluid. A sample calibration curve is shown in figure 8. A straight line was fit to the data, yielding a coefficient of determination (r^2) of 0.995.

Sprays were formed using a total of six separate fluids. They were formed from either mixtures of water and commercially available glycerine, or commercially available refined hydrocarbons (Texaco solvent neutral oils, SNO-100 and SNO-320, or Bennzoil Universal Calibration Fluid, UCF-1). Their compositions and physical properties are presented in table 1. Note that five of the fluids differ in viscosity (0.020, 0.040 or 0.080 Pa-s) and surface tension (either 0.030 Pa-m for 0.020 and 0.040 Pa-s or 0.067 Pa-m for all three viscosities). The sixth fluid was water. These viscosities and surface tensions were chosen to span the range of current alcohol-based consumer products and their (projected) water-based counterparts.

Fluid viscosities were measured using a Haake falling ball viscometer. Viscometer accuracy was checked using calibration oils having viscosities of 0.009 and 0.098 Pa-s. Measured values were within 5% of published data. Surface tensions were measured using a CSC model 70535 du-Nuoy ring tensiometer. The instrument was calibrated by placing a known weight on the ring and measuring the resulting force. Fluid densities were calculated from the quotient of a known volume of fluid and its measured weight. Volumes were measured using a graduated cylinder, while weights were measured using a Mettler model P1200N electronic balance.

The uncertainty in determining the entrainment number, E, was calculated using the expression developed by Bush (1994). Error in entrained mass flow rate measurements arises from the limited

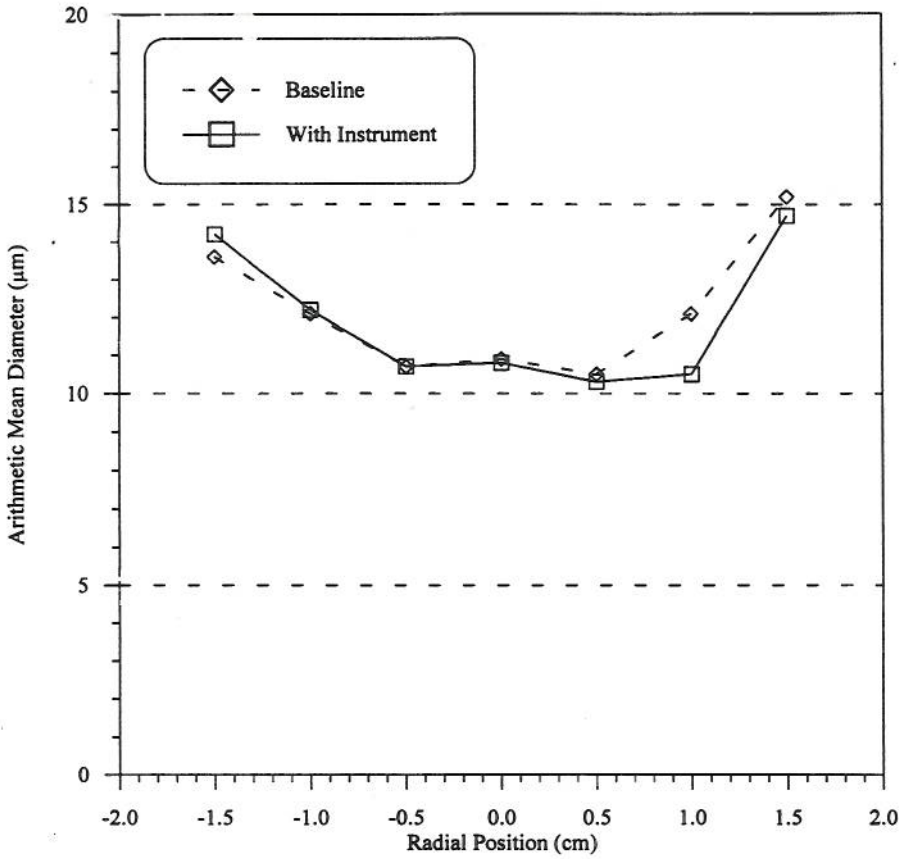

Figure 6. Number averaged droplet diameter (D_{10}) vs radial position for a ligament-controlled effervescent atomizer produced spray formed from a 0.080 Pa-s viscosity, 0.030 Pa-m surface tension fluid.

resolution of the micromanometer and is calculated as follows

$$\dot{m}_{err} = \frac{\pi}{4}\left[d_e^2 - (d_e - 2a)^2\right]\sqrt{2\rho(\Delta P)} + 2\rho^2 g(\Delta z) + \frac{\pi}{4}(d_e - 2a)^2\left[\frac{\Delta P}{v} + \frac{\rho g \Delta z}{v}\right] \quad [2]$$

where $\dot{m}_{err}$ is the error in the measured entrained air mass flow rate, d_e is the exit mask diameter, a is the annular gap between the edge of the exit mask and the edge of the spray drop sheath, ρ is the entrained air density, ΔP is the resolution limit of the micromanometer, g is the acceleration due to gravity, and v is the entrained air velocity.

The mass flow rate uncertainty calculated using this equation is as high as 30%. The only other significant source of uncertainty is associated with the momentum rate probe. This is approximately 7%, as noted by Bush *et al.* (1996). Assuming uncorrelated uncertainties, a value of 31% was calculated as the maximum overall uncertainty for the entrained mass flow rates.

3. RESULTS AND DISCUSSION

Normalized entrainment and momentum rate measurements were obtained using the entrainment device and momentum rate probe described above. Entrainment rate data are presented as normalized entrainment rate versus dimensionless axial distance. Normalized entrainment rate is defined as $\dot{m}_e/\dot{m}_L$, where $\dot{m}_e$ is the entrained air mass flow rate and $\dot{m}_L$ is the liquid mass flow rate. Dimensionless axial distance is defined as x/d_o, where x is the axial distance and d_o is the atomizer exit orifice diameter. Momentum rate results are plotted as momentum rate versus ALR. Six fluids, including water, were sprayed in order to determine the influence of operating conditions and fluid physical properties on the entrainment behavior and momentum rates of ligament-controlled effervescent atomizer produced sprays.

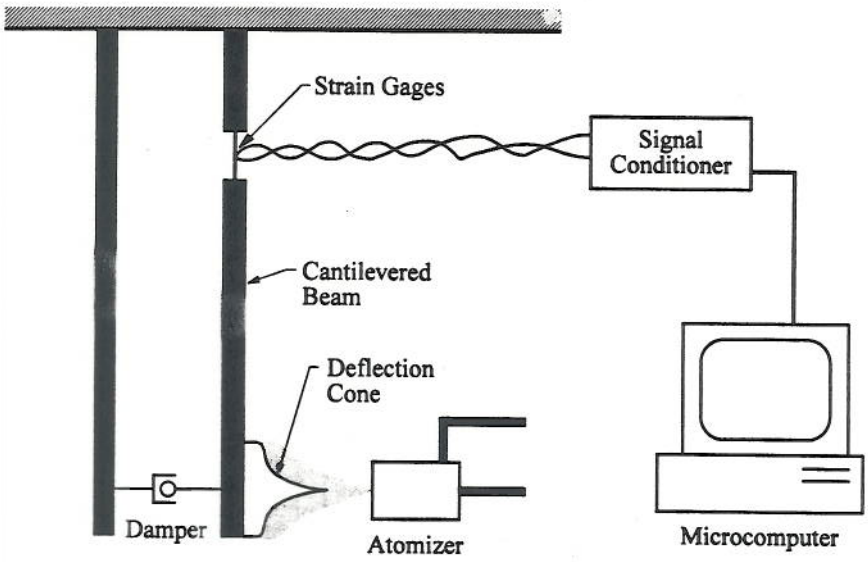

Figure 7. Momentum rate probe of Bush *et al.* (1996).

Bush (1994) reported normalized entrainment results for the Lund *et al.* (1993) "conventional" effervescent atomizer. His data showed that normalized entrainment measurements scaled linearly with dimensionless axial position, as was predicted by the dimensional analysis of Ricou and Spalding (1961). Normalized entrainment rates were also reported to increase with increasing

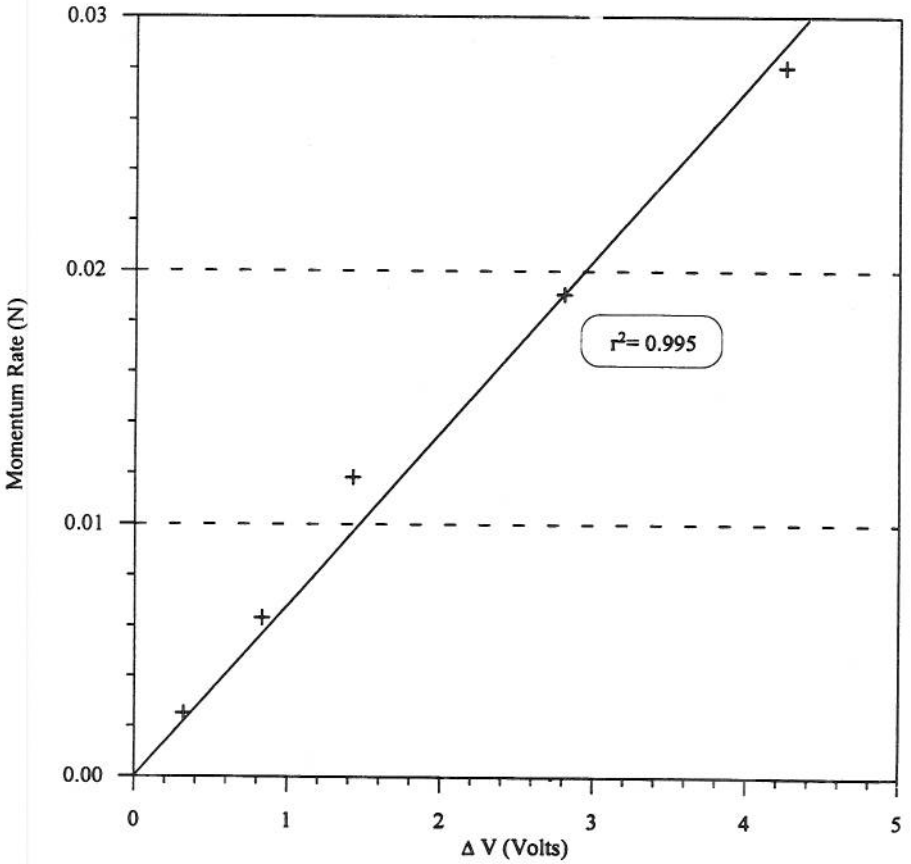

Figure 8. Calibration data for momentum rate probe of figure 7.

Table 1. Composition and physical properties of spray fluids (at room conditions)

Fluid number	Composition (weight %)	Viscosity (Pa-s)	Surface tension (Pa-m)	Density (kg/m^3)
1	63/37 Glycerine/water	0.020	0.067	1170
2	72/28 Glycerine/water	0.040	0.067	1197
3	80/20 Glycerine/water	0.080	0.067	1217
4	75/35 SNO 100/Bennzoil	0.020	0.030	840
5	90/10 SNO 100/SNO 320	0.040	0.030	847
6	Water	0.001	0.072	998

air-to-liquid mass flow ratio (ALR). Normalized entrainment rates, plotted against dimensionless axial distance for a 1.0 g/s water spray produced using a Lund *et al.* (1993) style atomizer, are shown in figure 9.

Figure 10 shows normalized entrainment rates versus dimensionless axial distance for a ligament-controlled effervescent atomizer spraying water under the same conditions as for figure 9. Again, normalized entrainment rates are found to scale linearly with dimensionless axial distance and to increase with increasing ALR ($r^2 \geq 0.984$ for all cases). These features are common to all normalized entrainment measurements for all liquids sprayed in this investigation. The ALR scaling, in particular, is not surprising since increasing ALR increases the exit momentum rate of the spray. In addition, increasing ALR results in a small, but noticeable (Sutherland 1996), decrease in mean drop size which should result in more effective momentum transfer from the spray to the surrounding air. The more effective momentum transfer is expected to increase entrainment.

When comparing the magnitudes of the normalized entrainment rates, values decreased upon changing from the Lund *et al.* (1993) atomizer to the ligament-controlled effervescent atomizer.

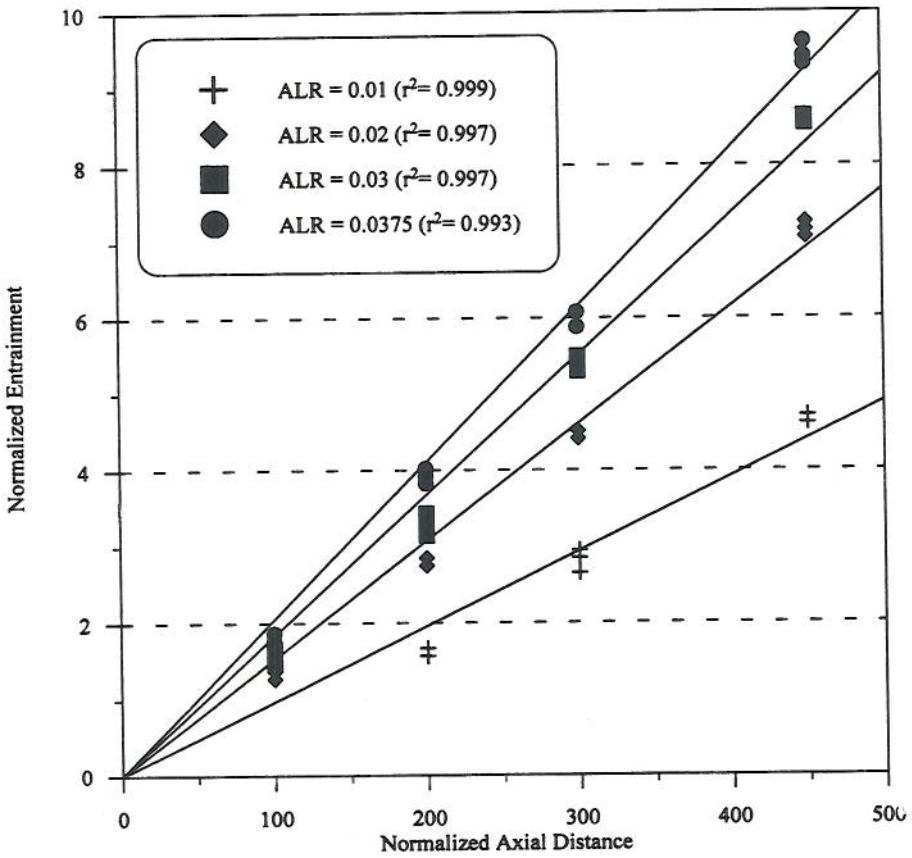

Figure 9. Normalized entrainment vs dimensionless distance for water being sprayed at a mass flow rate of 1.0 g/s using a conventional effervescent atomizer.

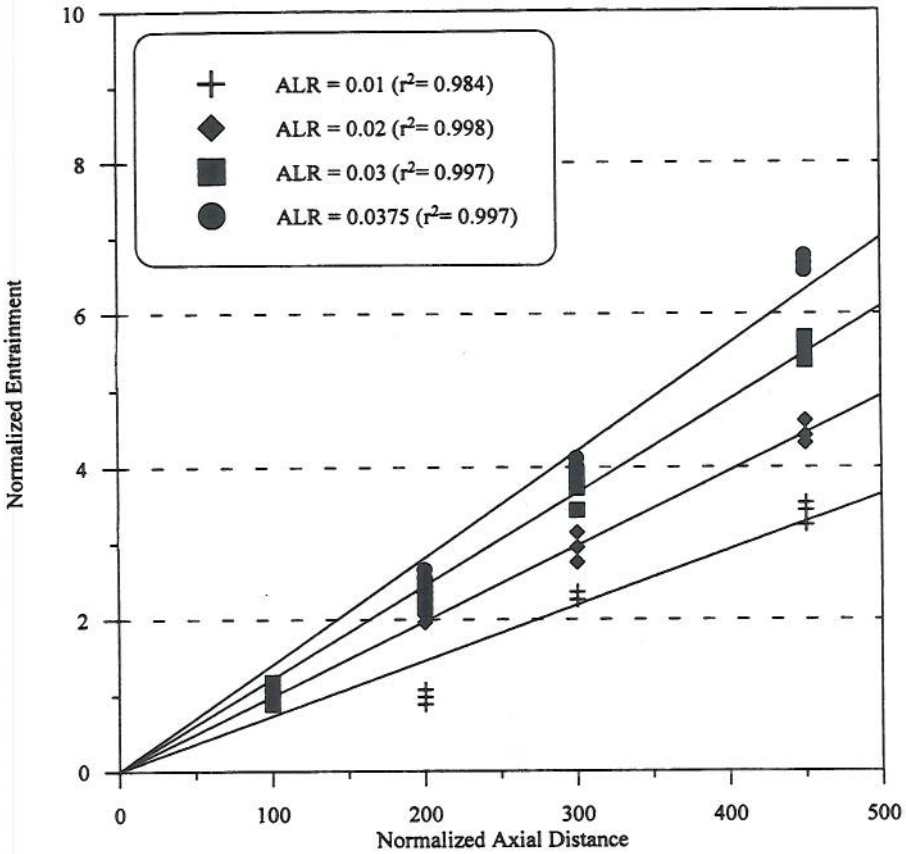

Figure 10. Normalized entrainment vs dimensionless distance for water being sprayed at a mass flow rate of 1.0 g/s using a ligament-controlled effervescent atomizer.

This is due to the dependence of entrainment behavior on the exit momentum rate of the spray. Unlike the Lund *et al.* (1993) atomizer, the ligament-controlled effervescent atomizer requires the two-phase flow to pass through a porous insert before exiting. This alters the near nozzle breakup structure and thus the exit momentum rate of the spray, thereby causing a change in the entrainment behavior. As will be demonstrated, the end result is a decrease in the dimensionless entrainment number, E.

Entrainment data for ligament-controlled effervescent atomizer produced sprays using working fluids other than water are presented in table 2. A representative plot is included as figure 11. Plots for the remaining fluids are reported by Sutherland (1996). The five fluids sprayed have surface tensions of 0.030 or 0.067 Pa-m and viscosities varying from 0.020 to 0.080 Pa-s. In each case, the data exhibit a linear relationship between normalized entrainment and normalized axial distance; the correlation coefficients range from 0.989 to 0.998. In addition, the slope of the

Table 2. Slopes and coefficients of determination for least squares linear fits to normalized entrainment vs normalized axial distance data for fluids sprayed at 0.6 g/s

↓Fluid/ALR→	0.075	0.1	0.015	0.02
1	0.0082, $r^2 = 0.998$	0.0097, $r^2 = 0.994$	0.012, $r^2 = 0.998$	0.015, $r^2 = 0.998$
2	0.0083, $r^2 = 0.998$	0.0091, $r^2 = 0.998$	0.011, $r^2 = 0.997$	0.014, $r^2 = 0.998$
3	0.0084, $r^2 = 0.989$	0.011, $r^2 = 0.996$	0.014, $r^2 = 0.997$	0.017, $r^2 = 0.998$
4	0.0081, $r^2 = 0.994$	0.0095, $r^2 = 0.993$	0.011, $r^2 = 0.998$	0.014, $r^2 = 0.997$
5	0.0081, $r^2 = 0.997$	0.0098, $r^2 = 0.996$	0.011, $r^2 = 0.996$	0.015, $r^2 = 0.998$

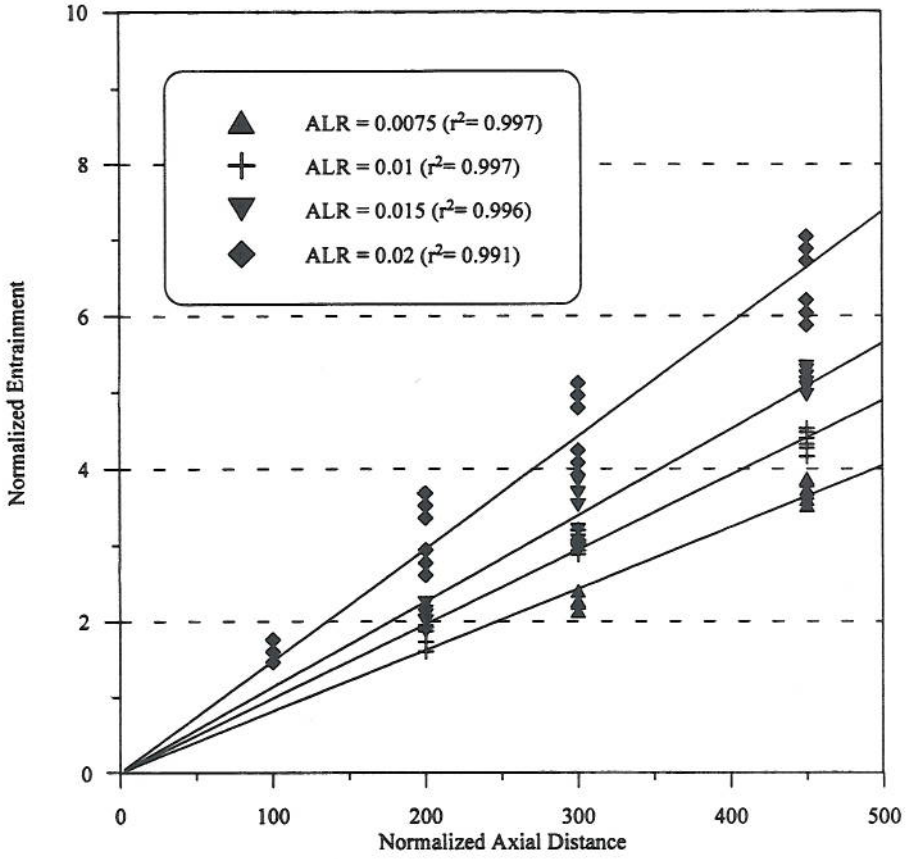

Figure 11. Normalized entrainment vs normalized axial distance for a fluid (fluid 5) having a viscosity of 0.040 Pa-s, a surface tension of 0.030 Pa-m, and operating at liquid mass flow rates of 0.5 and 0.6 g/s.

normalized entrainment vs normalized axial distance lines increases with ALR in all cases. This behavior is anticipated since an increase in ALR leads directly to an increase in exit orifice momentum rate.

The effect of viscosity on normalized entrainment rate is observed through comparison of data for fluids having similar surface tensions. Comparison of water data from figure 10 with that of fluids 1–3 (at equal ALRs) indicates an increase in normalized entrainment of 25–35% as viscosity is increased from 0.001 to 0.020 Pa-s, but a smaller effect on the normalized entrainment rates when the viscosity is 0.020 Pa-s or higher (normalized entrainment rates were within 16% of the mean for each ALR for viscosities between 0.020 and 0.080 Pa-s). Similar viscosity scaling is obtained from sprays having a common surface tension of 0.030 Pa-m, i.e. fluids 4 and 5—the data show that viscosity has little effect on the normalized entrainment rates for viscosities of 0.020 and 0.040 Pa-s, with variations being less 7% for each ALR.

The effects of surface tension can also be obtained from comparisons of table 2 data. The fluid 1 and 4 entries contain data from sprays with surface tensions of 0.067 and 0.030 Pa-m, respectively, and a common viscosity of 0.020 Pa-s. Comparison of these data indicates a slight decrease in normalized entrainment ($<12\%$ in all cases) with a decrease in surface tension. The fluid 2 and 5 entries contain data from sprays with surface tensions of 0.067 and 0.030 Pa-m, respectively, and a common viscosity of 0.040 Pa-s. Comparison of these data show little surface tension scaling; normalized entrainment rates are within 7% of each other. Since any scaling observed due to surface tension is small (well within experimental uncertainty), it can be concluded that surface tension has little effect on normalized entrainment rates for fluids with viscosities above 0.020 Pa-s.

Figure 11 presents entrainment data obtained at two different liquid mass flow rates (0.5 and 0.6 g/s). The data exhibit a linear dependence of normalized entrainment on dimensionless axial

distance ($r^2 \geq 0.990$ for all cases), as well as an increase in the slope of these lines with an increase in ALR. Most importantly, the data for both mass flow rates collapse to a single line for any particular ALR value.

Momentum rate data corresponding to the entrainment rate data of figures 10 and 11 and table 2 are presented in figures 12 and 13 and table 3, respectively. Figures 12 and 13 are representative of all momentum rate data obtained during this study and show that momentum rate is linearly proportional to ALR. Coefficients of determination (r^2) are above 0.962 in all cases.

Momentum rate for a water spray is plotted vs air-to-liquid mass flow ratio and shown in figure 12. When compared to data obtained by Bush (1994) at the same liquid mas flow rate, i.e. 1.0 g/s, the momentum rates for ligament-controlled effervescent atomizer produced sprays are lower over the entire range of air-to-liquid mass flow rate ratios. This supports the hypothesis that the addition of a porous insert does indeed alter the exit momentum of the spray and, ultimately, the entrainment behavior.

The influence of surface tension on momentum rate can be determined by comparing the fluid 1 and 4 or 2 and 5 entries in table 3. In both cases, momentum rates decrease when the surface tension is increased. This same trend was reported by Bush (1994) and was attributed to differences in liquid density, not surface tension. Lower liquid density results in a lower void fraction at the atomizer exit and, thus, higher interphase velocity slip. Higher slip results in a higher momentum rate.

The influence of viscosity on momentum rate is unclear. The fluid 1–3 entries in table 3 show momentum rates for liquids having viscosities of 0.020, 0.040 and 0.080 Pa-s, respectively, and a common surface tension of 0.067 Pa-m. An increase in viscosity from 0.020 to 0.040 Pa-s results in a decrease in momentum rate (slope), while a further increase in viscosity from 0.040 to 0.080 Pa-s

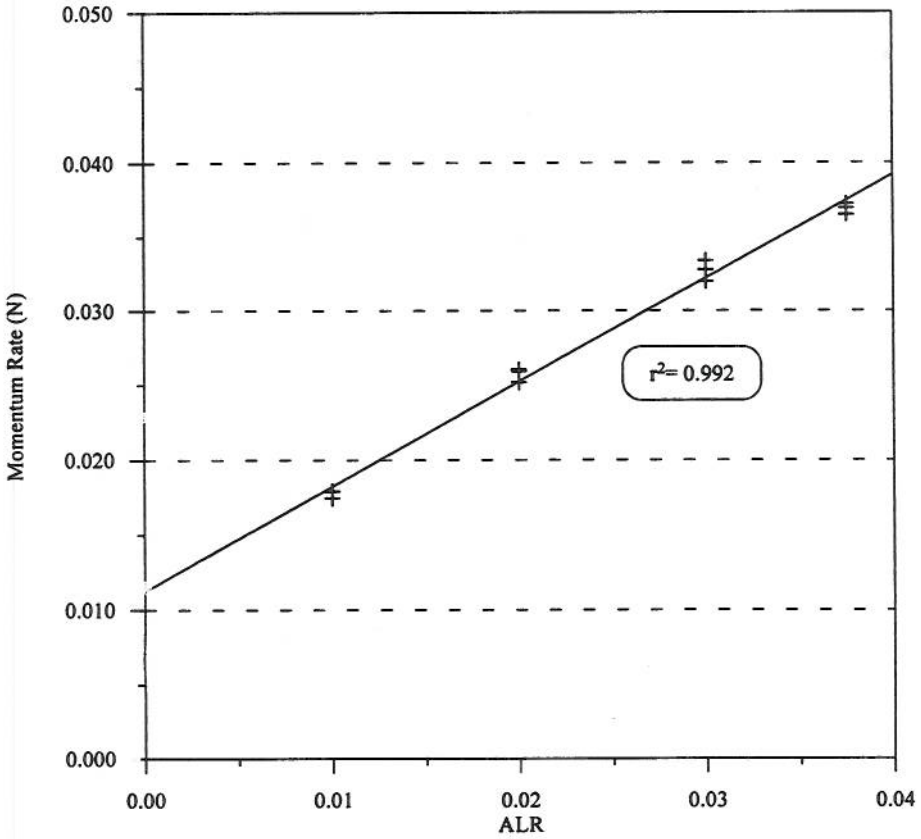

Figure 12. Momentum rate vs air–liquid ratio (ALR) for water.

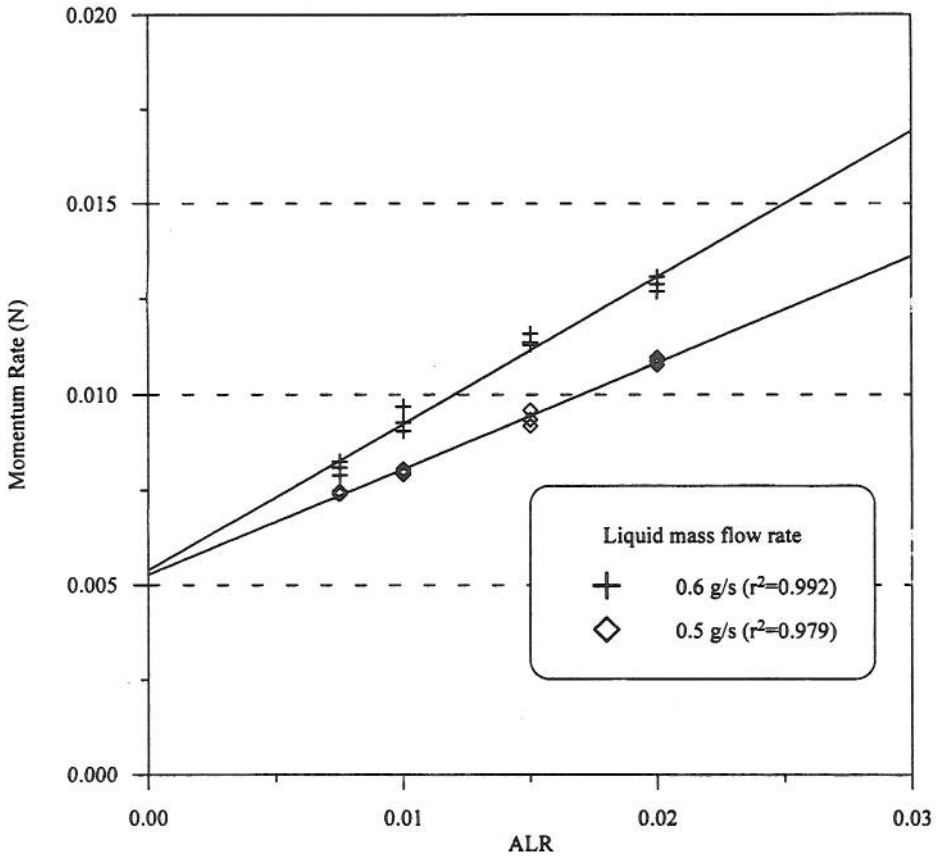

Figure 13. Momentum rate vs air–liquid ratio (ALR), at two mass flow rates, for a fluid (fluid 5) having a viscosity of 0.040 Pa-s and a surface tension of 0.030 Pa-m.

results in an increase in momentum rate (slope). The relative changes in momentum rate are small (~20%) and could be due to experimental uncertainty.

When examining the influence of viscosity on momentum rates for fluids with a common surface tension of 0.030 Pa-m, the effects are less obvious. The fluid 4 and 5 entries in table 3 contain data for mixtures having viscosities of 0.020 and 0.040 Pa-s, respectively, and operating at two liquid mass flow rates. These data show that momentum rate (slope) increases with viscosity at the low mass flow rate, yet exhibits only a minor variation with viscosity for the higher mass flow rate.

The effects of liquid mass flow rate on momentum rate may also be inferred from table 3. In each case, the momentum rate (slope) increases with an increase in liquid mass flow rate, from 0.17 to 0.37 for fluid 4 and from 0.28 to 0.38 for fluid 5. This is expected, since the momentum rate is expected to increase proportional to the liquid mass flow rate.

Table 3. Slopes, intercepts and coefficients of determination for least squares linear fits to momentum rate vs air–liquid ratio (ALR) data

Fluid @ mass flow rate	Slope, intercept; r^2
1@0.6 g/s	0.39, 0.0060; $r^2 = 0.998$
2@0.6 g/s	0.32, 0.0057; $r^2 = 0.993$
3@0.6 g/s	0.37, 0.0065; $r^2 = 0.962$
4@0.5 g/s	0.17, 0.0057; $r^2 = 0.992$
4@0.6 g/s	0.37, 0.0086; $r^2 = 0.989$
5@0.5 g/s	0.28, 0.0053; $r^2 = 0.992$
5@0.6 g/s	0.38, 0.0054; $r^2 = 0.979$

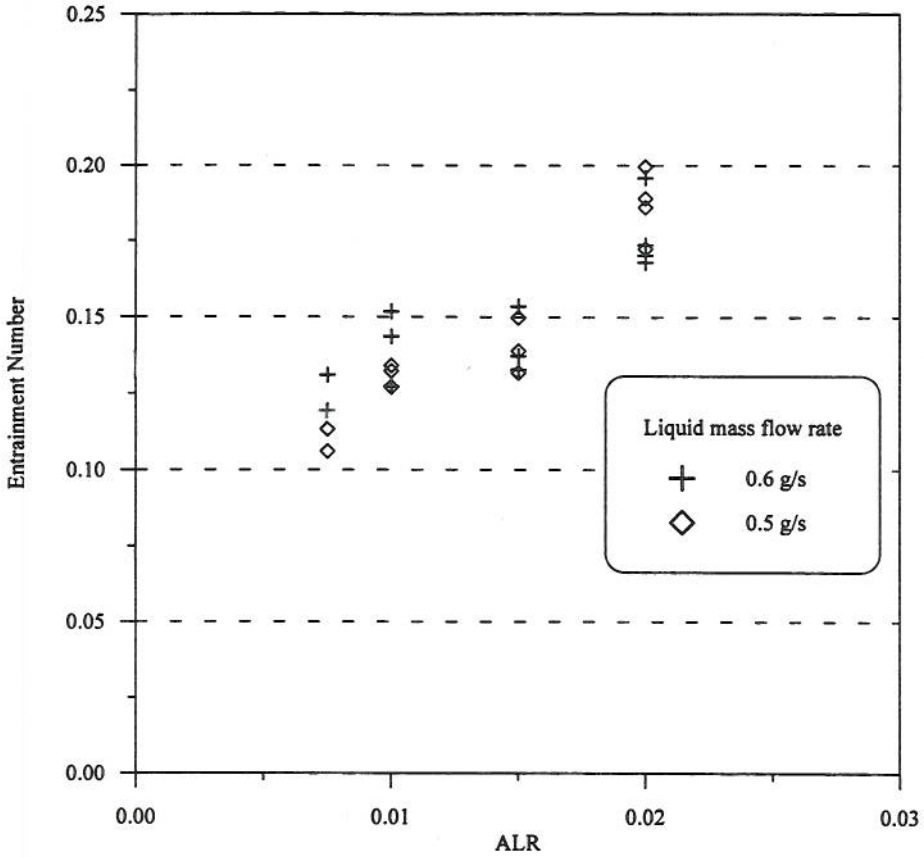

Figure 14. Entrainment number vs air–liquid ratio (ALR) for a fluid (fluid 5) having a viscosity of 0.040 Pa-s and a surface tension of 0.030 Pa-m, operating at two liquid mass flow rates.

The entrainment rate data were combined with the momentum rate data to calculate entrainment numbers using the model developed by Bush (1994). Bush's (1994) model is based on the work of Ricou and Spalding (1961), who employed a Buckingham Pi analysis using the exit momentum rate, entrained gas density, and axial distance as the normalizing parameters to obtain [1].

Entrainment numbers were calculated for five different fluids with varying viscosities and surface tensions by correlating experimental data via [1]. They are listed in table 4. A representative sample of the data is included as figure 14, while figure 15 is a composite of all the data acquired in this study (fluids 1–5, plus water).

Figure 14 shows entrainment number results for a water spray. A noticeable increase in entrainment number with air-to-liquid mass flow rate ratio is observed. This behavior occurred for all fluids considered during this investigation.

Inspection of figure 15 leads to the conclusion that air-to-liquid mass flow ratio has some influence on the value of the entrainment number. In all cases, the value of the entrainment number increases with increasing ALR. It might be argued that this variation is due to experimental uncertainty, since the entrainment number values differ from the mean by less than 40% in all cases, which is approximately the range of uncertainty involved in the calculation. However, consideration of the limiting cases of pure gas and pure liquid jets demonstrates some ALR scaling should be expected. For the pure gas jet, the entrainment number has been shown by Ricou and Spalding (1961) to be approximately 0.28. This is nearly twice the value reported here for ligament-controlled effervescent atomizer-produced sprays. For the pure liquid jet, the entrainment number would be zero, if defined to be equal to the amount of surrounding gas crossing the spray boundary, as it is in this study. If the entrainment number is instead defined to be proportional to the amount of surrounding gas set in motion by the liquid jet, a simple boundary layer analysis indicates that E would be approximately 0.02. This is less than 8% of the Ricou and Spalding (1961)

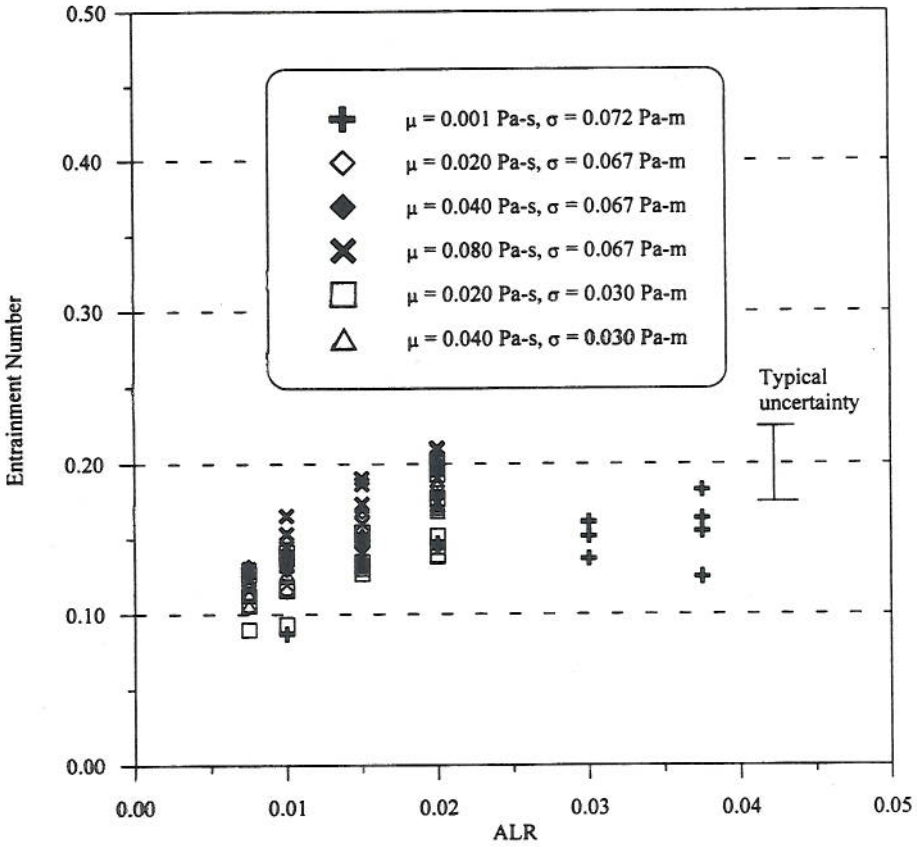

Figure 15. Entrainment number vs air/liquid ratio (ALR) for all fluids.

value and only 14% of the value reported here. Regardless of the approach taken to estimate the zero ALR limit for E, the conclusion is that E should increase with ALR.

Table 4 may be used to demonstrate the influence of the fluid physical properties on the entrainment number. A comparison of data from the fluid 1–3 entries, characteristic of water-based mixtures, indicates that entrainment number is relatively insensitive to fluid viscosity—average entrainment numbers differ by less than 15%. The lack of an influence of viscosity is also observed when comparing data from equal mass flow rate fluid 4 and 5 entries, which contain results characteristic of hydrocarbon-based mixtures—average entrainment numbers differ by less than 21%. This leads to the conclusion that fluid viscosity has a negligible impact on entrainment number throughout the range of conditions considered in this study.

The effects of surface tension on the entrainment number are demonstrated when comparing data from table 4 entries for fluid 1 with fluid 4 and for fluid 2 with fluid 5, all at equal mass flow rates. As can be observed, variations in mean entrainment number due to changes in surface tension are less than 4% and, therefore, well within experimental uncertainty of the mean value. This indicates that surface tension has little effect on entrainment number.

Table 4. Average entrainment numbers

Fluid	$E \pm 2\sigma$
1@0.6 g/s	0.158 ± 0.058
2@0.6 g/s	0.153 ± 0.053
3@0.6 g/s	0.175 ± 0.065
4@0.5 g/s	0.124 ± 0.040
4@0.6 g/s	0.153 ± 0.056
5@0.5 g/s	0.150 ± 0.046
5@0.6 g/s	0.148 ± 0.063

Figure 15 reinforces the conclusion that the entrainment number is insensitive to fluid physical properties, and also demonstrates that ALR does have an effect. Considering the data as a whole, the resulting value for E is 0.15 ± 0.056 (2σ). Note that 2σ corresponds closely to the uncertainty in these estimates ($\pm 30\%$). Also note that E values for all fluids sprayed under all combinations of liquid mass flow rates and ALR are within 40% of the mean value. Finally, since normalized entrainment scales linearly with normalized axial distance (to within our experiemntal accuracy), we conclude that the model accurately estimates entrainment in low air-to-liquid mass flow rate ratio, ligament-controlled effervescent atomizer-produced sprays.

The single E value reported here, for a wide range of conditions, is in contrast to the earlier results of Bush (1994), who noted that entrainment number depends on the liquid density and the diameter of the exit orifice for sprays produced by conventional effervescent atomizers. Bush (1994) attributed the observed scaling to a possible shift in the flow structure at the nozzle exit or a significant shift in mean drop size. These phenomena were not observed in this investigation and their absence may explain the similarity in the entrainment number for all fluids sprayed. The single value of E may also indicate that the current atomizer provides relatively steady sprays, in contrast to those produced by conventional effervescent atomizers (Luong 1996).

4. SUMMARY AND CONCLUSIONS

The results of this study are summarized as follows:

- Normalized entrainment by ligament-controlled effervescent atomizer produced sprays is linearly proportional to normalized axial distance, as has been reported for gas jets and for some other types of sprays.
- Normalized entrainment by these sprays increases with atomizing air-to-liquid mass flow rate ratio (ALR), as would be expected since an increase in ALR increases the initial momentum rate of the spray; entrainment data obtained at two liquid mass flowrates collapsed on to a common line.
- Liquid surface tension has a negligible effect on normalized entrainment; increasing liquid viscosity from 0.001 to 0.020 Pa-s increased normalized entrainment by approximately 30–50%, with further increases in liquid viscosity having a much smaller impact (less than 12%).
- The initial spray momentum rate is proportional to ALR and to liquid mass flow rate, as expected.
- Liquid surface tension had a negligible effect on momentum rate; the influence of viscosity was mixed with momentum rate increasing with an increase in viscosity in some cases and decreasing with an increase in viscosity in others.
- Entrainment number is relatively insensitive to liquid physical properties—all variations were within experimental uncertainty.
- Entrainment number increases with ALR, as would be expected by considering the limiting cases of pure liquid (ALR = 0) and pure gas (ALR = ∞) jets; the value of entrainment number determined here, 0.15 ± 0.056 (2σ), lies between the gas jet value, 0.282, reported by Ricou and Spalding (1961) and the liquid jet (issuing into air) value of 0.

The following conclusions can be drawn, based on the results of this study:

- Entrainment into steady two-phase jets where the gas and liquid streams exhibit interphase velocity slip can be modeled using the momentum rate approach of Ricou and Spalding (1961), although their entrainment number value is no longer applicable. The experimentally determined entrainment number for the two-phase jets studied here increases with ALR.
- The appropriate experimentally determined entrainment number, E, for ligament-controlled effervescent atomizer produced sprays is 0.15 ± 0.056 (2σ). This value of E predicts entrainment to within 40% for sprays considered in this study.
- Entrainment depends on the structure of the spray present at the atomizer exit, as shown by a comparison of results from this study with those of Bush (1994).

Acknowledgements—We thank our colleague Prof. J. P. Gore for advice given during many discussions about entrainment. This work was performed under EPA Cooperative Agreement No. CR822618. The technical monitor is Kelly W. Leovic.

REFERENCES

Benatt, F. G. S. and Eisenklam, P. (1969) Gaseous entrainment into axisymmetric liquid sprays. *Journal of the Institute of Fuel* **August,** 309–315.

Binark, H. and Ranz, W. E. (1958) Induced air flows in fuel sprays. ASME Paper No. 58-A-284 (1958 Annual Meeting of the ASME).

Boysan, F. and Binark, H. (1979) Predictions of induced air flows in hollow cone sprays. *Journal of Fluids Engineering* **101,** 313–318.

Briffa, F. E. J. and Dombrowski, N. (1966) Entrainment of air into a liquid spray. *AIChE Journal* **12,** 708–717.

Buckner, H. N. and Sojka, P. E. (1993) Effervescent atomization of high viscosity fluids. Part II: Non-Newtonian liquids. *Atomization and Sprays* **3,** 157–170.

Bush, S. G. (1994) Entrainment by effervescent sprays at low mass flow rates. MSME thesis, Purdue University.

Bush, S. G. and Sojka, P. E. (1994) Entrainment by effervescent sprays at low mass flow rates. Presented at the *6th ICLASS*, Rouen, France.

Bush, S. G., Bennett, J. B., Sojka, P. E., Panchagnula, M. V. and Plesniak, M. W. (1996) A momentum rate probe for use with two-phase flows. *Review of Scientific Instruments* **67,** 1878–1885.

Deichsel, M. and Winter, E. R. F. (1990) Adiabatic two-phase flow of air–water mixtures under critical flow conditions. *International Journal of Multiphase Flow* **16,** 391–406.

Geckler, S. C. and Sojka, P. E. (1995) Effervescent atomization of viscoelastic liquids. *Atomization and Sprays* (to appear).

Lefebvre, A. H., Wang, X. F. and Martin, C. A. (1988) Spray characteristics of aerated-liquid pressure atomizers. *AIAA J. Propulsion and Power* **4,** 293–298.

Lund, M. T., Sojka, P. E., Lefebvre, A. H. and Gosselin, P. G. (1993) Effervescent atomization at low mass flow rates. Part I: The influence of surface tension. *Atomization and Sprays* **3,** 77–89.

Luong, J. T. K. (1996) Unsteadiness in low mass flow rate effervescent atomizer produced sprays. MSME thesis, Purdue University.

MacGregor, S. A. (1991) Air entrainment in spray jets. *International Journal of Heat and Fluid Flow* **12,** 279–283.

Rasbash, D. J. and Stark, G. (1962) Some aerodynamic properties of sprays. *The Chemical Engineer* **December,** A83–A88.

Ricou, F. P. and Spalding, D. B. (1961) Measurements of entrainment by axisymmetric turbulent jets. *Journal of Fluid Mechanics* **11,** 21–32.

Roesler, T. C. and Lefebvre, A. H. (1989) Studies on aerated-liquid atomization. *International J. Turbo and Jet Engines* **6,** 221–230.

Rothe, P. H. and Block, J. A. (1977) Aerodynamic behavior of liquid sprays. *International Journal of Multiphase Flow* **3,** 263–272.

Ruff, G. A., Sagar, A. D. and Faeth, G. M. (1989) Structure and mixing properties of pressure-atomized sprays. *AIAA Journal* **27,** 901–908.

Santangelo, P. J. and Sojka, P. E. (1995) A holographic investigation of the near-nozzle structure of an effervescent atomizer-produced spray. *Atomization and Sprays* **5,** 137–155.

Sutherland, J. J. (1996) Ligament-controlled effervescent atomization. MSME thesis, Purdue University.

Tishkoff, J. (1985) Air entrainment into sprays from swirl chamber atomizers. *Proceedings 3rd ICLASS*, London, UK.

Wang, X. F., Chin, J. S. and Lefebvre, A. H. (1987) Influence of gas injector geometry on atomization performance of aerated-liquid nozzles. *Heat Tarnsfer in Furnaces*. ASME HTD, Vol. 74, pp. 11–18.

White, F. M. (1991) *Viscous Fluid Flow*, 2nd edn. McGraw-Hill, New York.

Whitlow, J. D. and Lefebvre, A. H. (1993) Effervescent atomizer operation and spray characteristics. *Atomization and Sprays* **3,** 137–155.